A Ripple Minimization Strategy for Direct Torque and Flux Control of Induction Motors using Sliding Modes*

M.E. Romero† Julio H. Braslavsky M.I. Valla‡

Ingeniería en Automatización y Control Industrial
Departamento de Ciencia y Tecnología
Universidad Nacional de Quilmes
Avenida Calchaquí 5800, F. Varela
1888 Buenos Aires, Argentina
http://iaci.unq.edu.ar

Informe Interno
Septiembre 2001

Abstract

We present a direct torque and flux control (DTFC) design for an electric induction motor using a sliding-mode control technique. A distinctive feature of our approach is that, by appropriately parameterizing and implementing the sliding-mode controller, we explicitely take into account the discontinuous nature of the actuator in the design process. As a result, we obtain an improved implementation of DTFC, which significantly reduces the number of commutations and the levels of steady-state ripple with respect to those typically obtained with conventional implementations of DTFC.

Keywords: Torque control, Sliding-mode control, Induction motors, Electrical machines, Steady-state errors.

1 Introduction

Vector control of electrical drives, with its two main commercial implementation approaches, Field Oriented Control (FOC) and Direct Flux and Torque Control (DTFC), has generated much discussion comparing advantages and disadvantages of each scheme [e.g., Le-Huy, 1995, Vas, 1998]. On one hand, FOC appears as having a better performance than DTFC in a wide range of speed and load conditions. However, the performance of a FOC implementation critically depends on very accurate coordinate transformations and flux angle estimation, which are complex. This complexity involves a significantly larger number of computations than the simpler alternative of an equivalent DTFC implementation, which normally only requires setting up a *lookup table* that specifies the actuation to a each given torque and flux condition.

On the other hand, the simplicity of DTFC contrasts with some performance limitations, which essentially arise from the way the inverter driving the motor operates in this approach. Namely,

1. The inverter operates at a variable switching frequency, and moreover, there is no control on the number of switches at a given update of the control signal.

*Submitted to the 15th IFAC World Congress, Barcelona, June 2002.

†Depto. de Electrónica, Universidad Nacional de Rosario, Riobamba 245 bis, (2000) Rosario, Argentina

‡Laboratorio de Electrónica Industrial, Control e Instrumentación, Universidad Nacional de La Plata, CC91 (1900) La Plata, Argentina

2. The inverter can only generate a restricted set of actuating signals for a range of operating conditions, for which the maximum DC bus is always applied, independently of the magnitude of the error signal or the load of the motor.

These characteristics give rise to difficulties in startup (machine magnetization) and increased levels of steady-state torque ripple.

Because the simplicity of DTFC is highly desirable in many applications, a number of recent works have suggested different strategies to circumvent its performance limitations. For example, Kazmierkowki and Kasprowicz [1995] have proposed the introduction of an additional carrier signal to the torque controller input to improve startup and low speed operation, while Takahashi and Noguchi [1997], Idris and Yatim [2000], J.Kang and Sul [1998] suggest double parallel PWM-Inverter, injection of dither signal, triangular signal, and calculation of optimal switching instant technique for the reduction of steady-state torque ripple.

In recent works, Yan et al. [2000] and Romero and Valla [2000] have proposed modified DTFC control schemes based on the *sliding-mode* control (SMC) design technique [Utkin, 1993]. A distinctive feature of the SMC of electrical drives is that the discontinuous nature of the actuator (the inverter) may be explicitely taken into account within the design process. Moreover, being SMC a Lyapunov-based design technique [Khalil, 1996, §13], it brings in the design process a powerful set of modern nonlinear control tools to further analyze and tune the control system.

In this paper, we propose extensions to the SMC scheme presented in Romero and Valla [2000]. Firstly, we propose a methodology to design the inverter DC-bus value to guarantee convergence of the SMC (§3). Secondly, we present two strategies for the implementation of the SMC to achieve a significant reduction of the steady-state torque ripple and the number of switches at each change of control action, in comparison those obtained using conventional DTFC schemes (§4). We discuss and compare these results in §5, illustrating the performance of the proposed controller on simulation experiments.

2 Background

2.1 Induction Motor Model

We consider the following standard state-space model of the induction motor [Krause et al., 1986],

$$\begin{aligned}
\frac{i_{qs}}{dt} &= \frac{1}{\alpha}\left[\beta i_{qs} + \omega_r \alpha i_{ds} - \frac{R_r}{M}\lambda_{qs} + \omega_r \frac{L_r}{M}\lambda_{ds}\right] - \frac{L_r}{\alpha M}V_q \\
\frac{i_{ds}}{dt} &= \frac{1}{\alpha}\left[\beta i_{ds} - \omega_r \alpha i_{qs} - \frac{R_r}{M}\lambda_{ds} - \omega_r \frac{L_r}{M}\lambda_{qs}\right] - \frac{L_r}{M}V_d \\
\frac{d\lambda_{qs}}{dt} &= -R_s i_{qs} + V_q \\
\frac{\lambda_{ds}}{dt} &= -R_s i_{ds} + V_d \\
\frac{\omega_r}{dt} &= \tau_e - B\omega_r - \tau_l,
\end{aligned} \tag{1}$$

in which the state variables, the stator currents i_{qs}, i_{ds}, and fluxes $\lambda_{qs}, \lambda_{ds}$, are set in a reference frame fixed to the stator. Here, $\tau_e = \frac{3}{2}n(i_{qs}\lambda_{ds} - i_{ds}\lambda_{qs})$ denotes the electric torque, with n being the number of pole pairs, τ_l is the load torque, and ω_r denotes the rotor speed (in electrical rad/s). The constants α and β are $\alpha = M - (L_s L_r)/M$ and $\beta = (L_s R_r + L_r R_s)/M$, where L_s, L_r, M are the stator, rotor, and mutual inductances, and R_s, R_r the stator and rotor resistances, respectively.

The input voltages V_q and V_d in the model (1) represent the projections of the motor phase voltages V_r, V_s, V_t driving the motor on the so-called q,d-plane, i.e.,

$$\begin{bmatrix} V_q \\ V_d \end{bmatrix} = K \begin{bmatrix} V_r \\ V_s \\ V_t \end{bmatrix}, \quad K = \frac{2}{3}\begin{bmatrix} 1 & -1/2 & -1/2 \\ 0 & -\sqrt{3}/2 & \sqrt{3}/2 \end{bmatrix}. \tag{2}$$

The phase voltages V_r, V_s, V_t are generated by the inverter that drives the motor. Since there are eight admissible combinations of the three pairs of switches of the inverter, the resulting voltage vector driving the motor has eight possible positions (Figure 1). Two of these positions are null vectors, and correspond to the three upper switches closed, V_7 or the three lower switches closed,V_0. The remaining six positions are the active (non null) values of the voltage vector, shown in the q,d-plane in Figure 2.

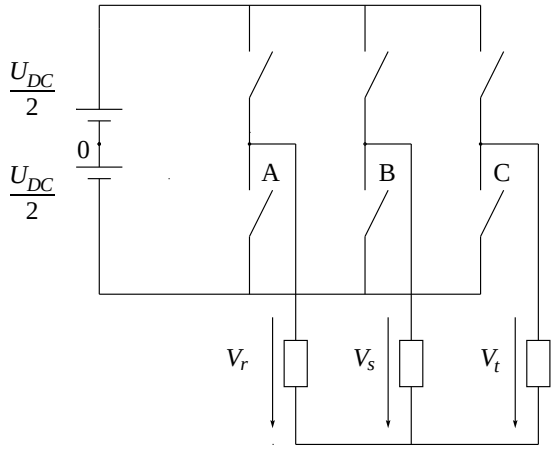

Figure 1: Inverter scheme.

Since there is usually no neutral connection between the motor and the inverter, the inverter leg voltages V_{A0}, V_{B0}, V_{C0} are not directly applied to the motor phases, but are related to them through the transformation

$$\begin{bmatrix} V_r \\ V_s \\ V_t \end{bmatrix} = \frac{1}{3} \begin{bmatrix} 2 & -1 & -1 \\ -1 & 2 & -1 \\ -1 & -1 & 2 \end{bmatrix} \begin{bmatrix} V_{A0} \\ V_{B0} \\ V_{C0} \end{bmatrix}. \tag{3}$$

Each of these leg voltages can only have two possible values, $\pm\frac{U_{DC}}{2}$, i.e., half of the *DC bus* U_{DC} (Figure 1).

2.2 DTFC control

DTFC is based on limit cycle control (hysteresis loops) of both electric torque and stator flux using the output voltage of the inverter. A *switching table* is used to select the best output voltage vector depending on the position of the stator flux and the desired action on electric torque and stator flux [Takahashi and Noguchi, 1986, Depenbrok, 1988]. The flux position in the q,d-plane is quantified in six sectors, one for each active voltage vector, $V_k, k = 1,2,\ldots,6$, as shown in Figure 2.

The switching table proposed in Takahashi and Noguchi [1986] is shown in Table 2.2. Alternative tables exist for specific operation modes, e.g., high/low speed operation, two-/four-quadrant operation [Buja et al., 1998].

3 Sliding Mode Control

The SMC strategy is based on the design of a discontinuous control signal that drives the system towards special manifolds in the state-space. These manifolds are chosen in a way that the system will have the desired behavior as the state converges to them [e.g., Utkin, 1993, Khalil, 1996].

We now review the basic strategy of SMC for an induction motor, as in Romero and Valla [2000], and show how to compute the inverter DC-bus U_{DC} *off-line* to guarantee the desired performance of the system in steady-state.

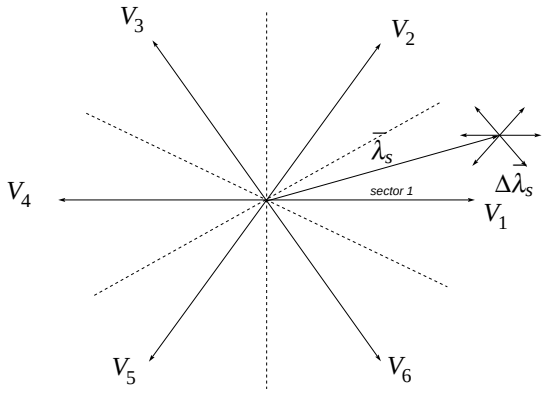

Figure 2: Active voltage vectors, stator flux vector, and sectors on the q,d-plane.

Desired Effect		Voltage vector depending on sector					
		1	2	3	4	5	6
$\lambda_s \uparrow$	$\tau_e \uparrow$	V_2	V_3	V_4	V_5	V_6	V_1
	$\tau_e -$	V_7	V_0	V_7	V_0	V_7	V_0
	$\tau_e \downarrow$	V_6	V_1	V_2	V_3	V_4	V_5
$\lambda_s \downarrow$	$\tau_e \uparrow$	V_3	V_4	V_5	V_6	V_1	V_2
	$\tau_e -$	V_0	V_7	V_0	V_7	V_0	V_7
	$\tau_e \downarrow$	V_5	V_6	V_1	V_2	V_3	V_4

Table 1: DTFC Table; $x \uparrow$: increase in x, $x \downarrow$: decrease in x, and $x-$: x remains invariant.

3.1 Basic Strategy

As in Romero and Valla [2000], we neglect the rotor speed dynamics as compared to the machine electrical dynamics, and consider ω_r in (1) constant for the synthesis process. On writing V_q, V_d in terms of V_{A0}, V_{B0}, V_{C0} using (2) and (3), system (1) may be represented in the form

$$\frac{dx}{dt} = Ax + Bv, \quad \text{where} \quad x = \begin{bmatrix} \lambda_{qs} & \lambda_{ds} & i_{qs} & i_{ds} \end{bmatrix}^T$$

and

$$v = \begin{bmatrix} V_{A0} & V_{B0} & V_{C0} \end{bmatrix}^T. \tag{4}$$

We postulate the SMC manifolds

$$S \triangleq \begin{bmatrix} S_1(x) \\ S_2(x) \\ S_3(v) \end{bmatrix} = \begin{bmatrix} (\lambda_{qs}^2 + \lambda_{ds}^2)/\lambda_{\text{ref}}^2 - 1 \\ \frac{3}{2} n (i_{qs}\lambda_{ds} - i_{ds}\lambda_{qs})/\tau_{\text{ref}} - 1 \\ \int (V_{A0}(t) + V_{B0} + V_{C0}(t)) dt \end{bmatrix} = 0,$$

where λ_{ref} and τ_{ref} are the references for the flux magnitude and the torque. The manifold $S_1(x) = 0$ represents the tracking of the flux magnitude, the manifold $S_2(x) = 0$ represents the torque regulation, and the manifold $S_3(v) = 0$ represents a voltage balance condition for the inverter.

In Romero and Valla [2000] the candidate Lyapunov function $W = \frac{1}{2} S^T S \geq 0$ is proposed to achieve convergence to the manifolds $S = 0$. The time derivative of W along the system trajectories can be written as

$$\frac{dW}{dt} = S^T \frac{dS}{dt} = S^T (H + Dv), \tag{5}$$

where

$$H \triangleq \frac{\partial S}{\partial x} Ax + \begin{bmatrix} \frac{\partial S_1}{\partial t} \\ \frac{\partial S_2}{\partial t} \\ 0 \end{bmatrix} \text{ and } D \triangleq \frac{\partial S}{\partial x} B + \begin{bmatrix} 0 \\ 0 \\ \frac{\partial S_3}{\partial t} \end{bmatrix}. \tag{6}$$

To guarantee the convergence of the system states to the manifolds $S = 0$, an appropriate discontinuous control signal has to be chosen to make $dW/dt < 0$.

Because the inverter produces the three independent voltages V_{A0}, V_{B0}, V_{C0}, each of which, in turn, can only take the values $\pm U_{DC}/2$, it is natural to propose the discontinuous control signal v from (4) as

$$v = -U_0 \operatorname{sign}(S^*), \quad \text{with} \quad S^* \triangleq D^T S. \tag{7}$$

Now, on replacing (7) in (5) and rearranging terms, U_0 appears as the design parameter in

$$\begin{aligned} \frac{dW}{dt} &= S^T D D^{-1} H - S^T D U_0 \operatorname{sign}(S^*) \\ &= (S^*)^T H^* - U_0 |S^*|, \end{aligned} \tag{8}$$

where $H^{*T} \triangleq (D^{-1}H)^T = \begin{bmatrix} h_1^* & h_2^* & h_3^* \end{bmatrix}$ and $|S^*| = |S_1^*| + |S_2^*| + |S_3^*|$. Hence, from (8), by selecting U_0 such that

$$U_0 > |h_i^*|, \quad \forall i = 1, 2, 3, \tag{9}$$

convergence to the manifolds $S = 0$ is guaranteed [Utkin, 1993].

3.2 DC-Bus Design

We need to satisfy (9), where h_i^* is a *time-varying function*, with U_0 provided by the *constant* DC-bus $U_{DC}/2$. Hence, we propose to select U_0 as the worst-case value under steady-state conditions. To this purpose, we now determine a steady-state expression of $H^* = D^{-1}H$.

Let the reference values λ_{ref} and τ_{ref} be constant. By neglecting ripple, the flux and currents in (1) may be assumed as sinusoidal with phase, say $\theta(t)$. Furthermore, by neglecting leakage flux, the flux λ_{ds} and the current i_{ds} may be considered to be in phase, and the same occurs with λ_{qs} and i_{qs}. Under these hypotheses, $H = [h_1 \ h_2 \ h_3]^T$ in (6) turns out to be a constant vector given by

$$\begin{aligned}
h_1 &= -2R_r(i_{ds}\lambda_{ds} + i_{qs}\lambda_{qs})/\lambda_{\text{ref}} \\
&= -\frac{2R_r}{\lambda_{\text{ref}}}(i_{\max}\sin\theta\,\lambda_{\max}\sin\theta + i_{\max}\cos\theta\,\lambda_{\max}\cos\theta) \\
&= -2R_r i_{\max}\,\lambda_{\max}/\lambda_{\text{ref}}, \\
h_2 &= \frac{\beta}{\alpha}(i_{qs}\lambda_{ds} - i_{ds}\lambda_{qs}) + \omega_r(i_{ds}\lambda_{ds} + i_{qs}\lambda_{qs}) \\
&\qquad + \frac{\omega_r L_r}{\alpha M}(\lambda_{ds}^2 + \lambda_{qs}^2) \\
&= \frac{\beta}{\alpha\gamma}\tau_{\text{ref}} + \omega_r i_{\max}\lambda_{\max} + \frac{\omega_r L_r}{\alpha M}\lambda_{\text{ref}}^2, \\
h_3 &= 0.
\end{aligned}$$

On the other hand D in (6) can be shown to be

$$D = \Lambda * K \tag{10}$$

where K is given in (2), and

$$\Lambda = \begin{bmatrix} 2\lambda_{qs} & 2\lambda_{ds} & 0 \\ -\gamma[i_{ds} + \frac{L_r}{\alpha L_{sr}}\lambda_{ds}] & \gamma[i_{qs} + \frac{L_r}{\alpha L_{sr}}\lambda_{qs}] & 0 \\ 0 & 0 & 2 \end{bmatrix}.$$

Because, as mentioned before, λ_{ds} and i_{ds} are sines, and λ_{qs} and i_{qs} cosines, the (periodically time-varying) matrix Λ performs a rotation, i.e., a change of coordinates from a fixed (q,d)-frame to a $(q,d)^\omega$-frame rotating at the synchronous frequency $\omega = d\theta/dt$. Then *the matrix $D = \Lambda * K$ transforms the three phase magnitudes in the (R,S,T) frame, to a rotating frame oriented with $\lambda_s = [\lambda_{qs} \ \lambda_{ds}]^T$*. Notice that D is orthogonal, i.e., $D^T = D^{-1}$.

In summary, under steady-state conditions, the components of $D^{-1}H$ are three identical sinusoids shifted $2/3\pi$ rad each. We can then select $U_{DC} = 2U_0$ from

$$U_0 = \max_t \|D^{-1}H\|_\infty, \tag{11}$$

which may be easily computed *off-line*.

4 Implementations for Torque Ripple Reduction

This section presents the main contributions of the paper, namely, two techniques to implement the *on-line* computation of the control signal to achieve reduction of the steady-state torque ripple.

4.1 Lyapunov-Based Softening of the Control Action

The proposed constant value of U_0 in (11) has been shown to guarantee, in steady-state, the Lyapunov condition $dW/dt < 0$ required by SMC. However, notice from (8) that when $(S^*)^T H^* < 0$, this condition would still be guaranteed with $U_0 = 0$. This observation suggests the possibility of making the control voltage v a null voltage vector, V_0 or V_7, in that case, i.e.,

$$v = \begin{cases} -U_0 \operatorname{sign}(S^*) & \text{if } (S^*)^T H^* \geq 0, \\ V_0, V_7 & \text{otherwise.} \end{cases} \tag{12}$$

Such a design for the output of inverter requires the *on-line* computation of the value $(S^*)^T H^* = SH$. This computation, however, is not exceedingly complex and produces a significant reduction of torque ripple with respect to the basic SMC strategy of §3 or other conventional DTFC strategies. We further discuss and illustrate this point with simulations in §5.2.

4.2 Periodic Intersample Modulation by Averaging

When the control voltage v in (12) does need to be an active voltage vector, $V_k, k = 1, \ldots, 6$, the proposed SMC strategy applies the full U_0, which we have designed in §3.2 as a worst-case value to satisfy (9) under steady-state conditions. This worst-case value turns out to be particularly conservative at low frequencies, producing a growth of torque ripple.

Since the implementation of the controller is in discrete time, $t = NT_s, N = 0, 1, 2, \ldots$, with a control update time T_s, we propose to perform a *periodic modulation* of the applied voltage vector during the intersample period $[NT_s, (N+1)T_s)$ to further reduce the torque ripple when U_0 is too large. This modulation consists in applying the computed active voltage vector only on the first fraction of the intersample period $[NT_s, NT_s + T_{av})$, while assigning a null voltage vector V_0 or V_7 for the rest of the period $[NT_s + T_{av}, (N+1)T_s)$. The time T_{av}, which varies at each sampling time, is computed following an averaging procedure similar to that proposed in J.Kang and Sul [1998], as we see next.

We start by computing a virtual "necessary" voltage vector, say U_{0n}, to satisfy (9). At the sampling time $t = NT_s$, the value U_{0n} is obtained computing the "necessary" column voltages as

$$\begin{bmatrix} U_{0nA}(NT_s) & U_{0nB}(NT_s) & U_{0nC}(NT_s) \end{bmatrix}^T = H^*(NT_s). \tag{13}$$

Then, from (13) we obtain the magnitude of the voltage vector as (for simplicity we omit the argument (NT_s))

$$\|U_{0n}\|_2 = \sqrt{U_{0nq}^2 + U_{0nd}^2}, \qquad \text{with}$$

where

$$U_{0nq} = \frac{2}{3}(U_{0nA} - U_{0nB}/2 - U_{0nC}/2),$$
$$U_{0nd} = \frac{\sqrt{3}}{3}(U_{0nC} - U_{0nB}).$$

The implementation of U_{0n} is carried out by "averaging" active and null vectors, which may be represented by the expression

$$U_{0n} = \frac{T_{av} V_k + (T_s - T_{av}) V_0(V_7)}{T_s},$$

where T_{av} is defined as

$$T_{av} = \frac{\|U_{0n}\|_2}{\frac{2}{3} U_{DC}} T_s.$$

The active vector $V_k, k = 1,2,\ldots,6$ is provided by the control law (7), and the selection of the null vector V_0 or V_7 depends on the applied active vector in order to produce the least number of switch commutations. The quantity $\frac{2}{3}U_{DC}$ is the maximum magnitude of the voltage vector when an active vector is applied during the complete intersample interval $[NT_s,(N+1)T_s)$.

In summary, the proposed modulated control law v is given by

$$v(t) = \begin{cases} -U_0 \operatorname{sign}(S^*) & \text{if } SH \geq 0 \text{ and } NT_s \leq t < NT_s + T_{av}), \\ V_0, V_7 & \text{otherwise,} \end{cases}$$

$$\text{for } t \in [NT_s,(N+1)T_s). \quad (14)$$

5 Discussion and Simulation Results

This section discusses the performance of the proposed control (14), showing its advantages with respect to the basic scheme of §3.1 and conventional DTFC. We present simulation results that illustrate performance on

- Machine magnetization.
- Steady-state torque ripple.
- Switch commutations at control updates.

5.1 Machine Magnetization

The proposed control scheme (14) permits the machine magnetization without a torque reference signal, a feature that is not possible with a conventional DTFC scheme. This feature is possible because the proposed scheme can use all eight voltage vectors instead of the five admissible in conventional DTFC. The best choice for machine magnetization is the voltage vector which is collinear to the flux vector in each sector, namely, if the flux vector is in sector k, the best choice is V_k. This situation is not contemplated in conventional DTFC. Figure 3 shows the response of the proposed SMC scheme at start up. Because the proposed control law is not defined at the origin, however, it does require non zero initial conditions for start-up, which were set in $[\lambda_{qs}\ \lambda_{ds}] = [10^{-5}\ 0]$, i.e., the flux vector is in sector $k = 1$, and vector V_1 is selected to magnetize the machine.

5.2 Torque Ripple

By implementation of the softening of the control action of § 4.1 and the periodic modulation of § 4.2, the proposed control scheme achieves significant reduction of the steady-state torque ripple, as compared with the basic SMC and conventional DTFC schemes.

The ripple phenomenon in DTFC is mainly generated by two factors: (i) conventional DTFC assigns a single voltage vector for the whole sector, and (ii) voltage vectors producing torque decrease have a stronger action than those that produce torque increase.

The assignment of a single voltage vector to a whole sector in DTFC amounts to computing the control action based on an error measurement that is *quantized by sectors*. This quantization of the error by sectors may produce undesirable effects depending on whether the flux vector is at the beginning, in the middle, or at the end of the sector [Bertoluzzo et al., 1999]. A control action suitable when the flux vector is, for example, in the middle of the sector, could be inappropriate at the beginning.

A more appropriate strategy would take into account the position of the flux vector disregarding such a quantization by sectors. The proposed SMC naturally fulfills this requirement. Indeed, we can see from the expression of the control signal (7) that the information contained in $S^* = D^T S$ is the flux and torque error per phase, explicitely parameterized by the position of the stator flux vector. Because the matrix D^T performs a rotation from the $(q,d)^\omega$ coordinates to the (R,S,T) coordinates, we see that for a given value of S, the control

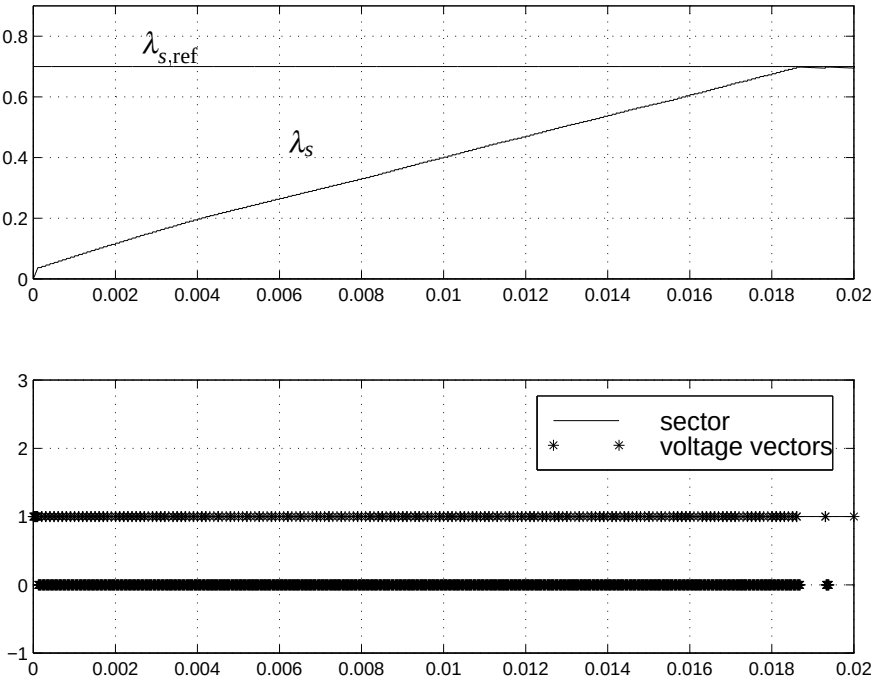

Figure 3: Reference and flux module at start up.

decision will depend on the position of the flux space vector. In this sense, the proposed strategy behaves like a FOC strategy.

The asymmetrical effect of voltage vectors in torque decrease or increase is discussed in Casadei et al. [1997]. Basically, any increase of torque $\Delta\tau_e = \tau_e(t_{N+1}) - \tau_e(t_N)$ has always a negative contribution (independently of the voltage input), a situation that becomes worse as speed and load torque go up.

In the proposed SMC strategy (14), the quantity $S^*H^* = SH < 0$ contains the information about when it is necessary to decrement the torque in $S_2 > 0$. In that case, a null vector V_0, (V_7) is selected as a control action, which results in an important decrease of torque ripple. Since H includes information about the references and their derivatives, a torque inversion, if required, is performed using active vectors, which makes the proposed control scheme suitable for four-quadrant operation. This operational makes our strategy better than those cited in Buja et al. [1998] as State Table A and B, which propose null vectors to decrement flux and torque (in case of torque inversion, these strategies will just apply null vectors, so that the motor will reverse the torque only with its unforced dynamics). Figure 4 shows the torque ripple in the conventional DTFC (top) and the proposed SMC scheme (bottom). The torque ripple produced by the proposed strategy is about half that of conventional DTFC. The simulation conditions are nominal speed and no load, with $T_s = 10^{-4}s$, a DC-bus $U_{DC} = 500$V, and motor parameters given by Table 2.

$R_s = 7\Omega$	$M = .1094$Hy
$R_r = 6.4\ \Omega$	$J = .0195$Nm/s^2
$L_s = .1289$Hy	$B = .002$
$L_r = .1289$Hy	$n = 2$

Table 2: Motor parameters for simulations.

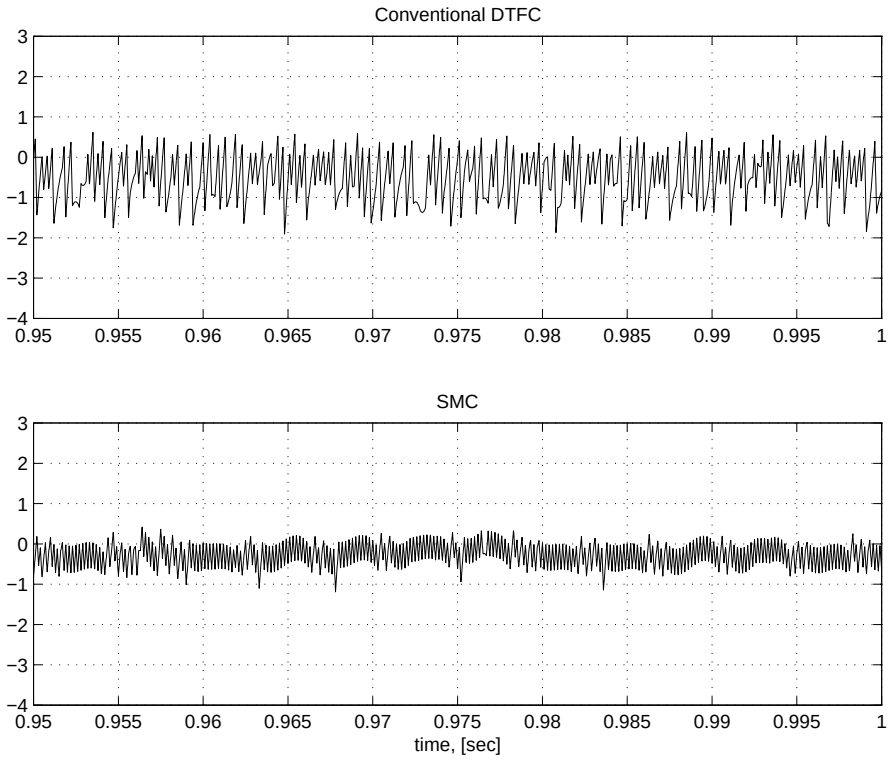

Figure 4: Torque ripple for conventional DTFC and SMC.

5.3 Switch Conmutations at Control Updates

The proposed control squeme (14) improves the inverter operation, because less number of switch conmutation are produced at each control update step. This improvement is achieved because the controller provides the switch configuration and the magnitud of the voltage vector necessary to drive the motor to $S = 0$, which is implemented by averaging technique of § 4.2. The resulting effect is that the deviations from $S = 0$ become smaller than those produces when the full DC-bus is applied during the complete intersample interval. Moreover, the correction actions can be done with voltage vectors that involve only one switch conmutation from one configuration to another (i.e., no oposite voltage vectors are selected). Figure 5 shows the number of switch conmutation at each control update step in the same simulation experiment of Figure 4.

6 Conclusions

We have presented a DTFC strategy using the SMC approach implementation for torque ripple reduction, namely, the use of null vectors to correct special error conditions, and a periodic modulation tecnique to apply the correct magnitud of the control signal. This methodology presents substantial advantages over conventional DTFC, namely, fixed frequency inverter operation, the possibility of machine magnetization without a torque reference signal, more control degrees of freedom, and use of (non quantized) flux space vector information in the control computation.

References

M. Bertoluzzo, G. Buja, and R. Menis. Analytical formulation of the direct control of induction motor drives. In *IEEE-Int. Symp. Industrial Electronics*, pages Ps14–Ps20, Bled, Slovenia, 1999.

G. Buja, D. Casadei, and G. Serra. Direct stator flux and torque control of an induction motor: theorethical

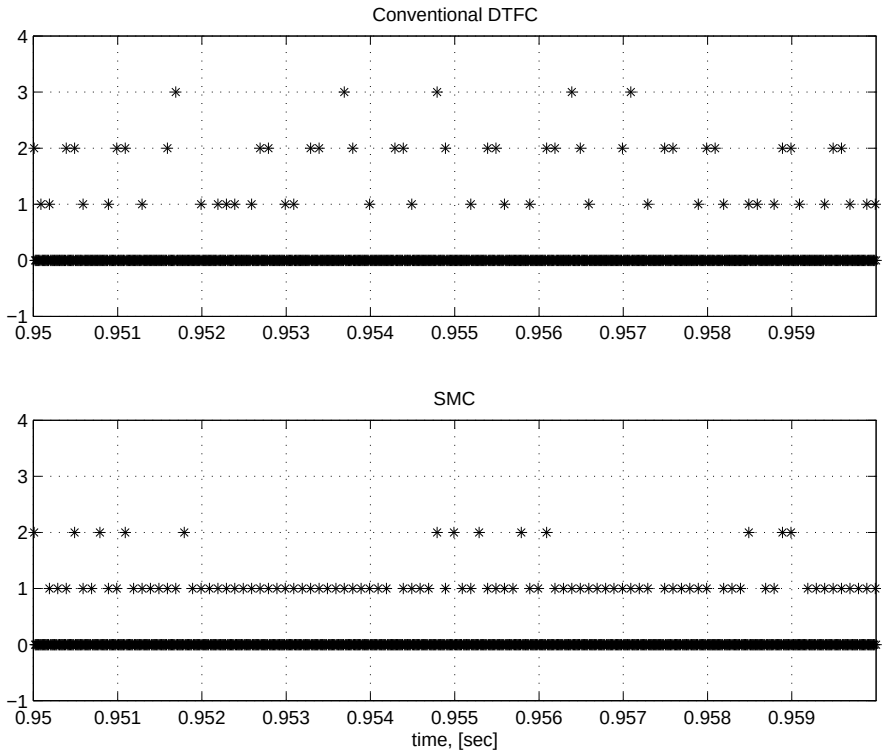

Figure 5: Number of switch commutations at each control update.

analysis and experimental results. In *IEEE Proc. Industrial Electronic Conf.*, pages T50–T64, Aachen, Germany, 1998.

D. Casadei, G. Serra, and A. Tani. Analitical investigation of torque and flux ripple in dtc scheme for induction motors. In *IEEE Proc. of Industrial Electronic Conf., IECON'97*, pages 552–556, New Orleans, USA, 1997.

M. Depenbrok. Direct Self-Control (DSC) of Inverter-Fed Induction Machine. *IEEE Trans. on Power Electronics.*, 3:420–429, 1988.

N. Idris and A. Yatim. Reduced torque ripple and constant switching frequency strategy for direct torque control of induction machine. In *IEEE Appl. Power Electronics Conf.*, pages 154–160, New Orleans, USA, 2000.

J.Kang and S. Sul. Torque ripple minimazation strategy for direct torque control of induction motor. In 33^{rd} *Annual Meeting Industrial Applications Soc., IEEE-IAS'98, Oct. 98*, pages 546–551, St. Louis, USA, 1998.

M. Kazmierkowki and A. Kasprowicz. Improve Direct Torque and Flux Vector Control of PWM Inverter-Fed Induction Drives. *IEEE Trans. Industrial Electronics.*, 42:344–349, 1995.

H. K. Khalil. *Nonlinear systems*. Prentice-Hall, 2nd edition, 1996.

P. Krause, O. Wasynnczuc, and S. Sudhoff. *Analysis of Electric Machinery*. McGraw-Hill, 1986.

Hoang Le-Huy. Comparison of field oriented control and direct torque control for induction motor drives. *No se*, 44:35–46, 1995.

M. Romero and M.I. Valla. DTFC of induction motor with sliding-mode approach. In *IEEE Int. Symp. Industrial Electronics*, pages 1287–1297, Cholula, Mexico, 2000.

I. Takahashi and T. Noguchi. A New Quick response and High -Efficiency Control Strategy of an Induction Motor. *IEEE Trans. Industry Appl.*, 22:820–827, 1986.

I. Takahashi and T. Noguchi. Take a look back upon the past decade of direct torque control. In *IEEE Proc. of Industrial Electronic Conf.*, pages 546–551, New Orleans, USA, 1997.

Vadim Utkin. Sliding mode control design principles and application to electrical drives. *IEEE Trans. Ind. Electron.*, 40:23–36, 1993.

Peter Vas. *Sensorless Vector Control and Direct Torque Control*. Oxford University Press, 1998.

Z. Yan, C. Jin, and V. Utkin. Sensorless Sliding-Mode Control of Induction Motors. *IEEE Trans. Ind. Electron.*, 47:1287–1297, 2000.